Anisotropy of creep deformation rate in hot-pressed Si_3N_4 with preferred orientation of the elongated grains

S. Y. YOON, T. AKATSU, E. YASUDA
Research Laboratory of Engineering Materials, Tokyo Institute of Technology, 4259 Nagatsuta, Midori, Yokohama, 226, Japan

Compressive creep deformation of hot-pressed silicon nitride with two different preorientations of grain was investigated at temperatures in the range of 1300–1400 °C under 30–100 MPa. The stress exponent of the creep rate was determined to be nearly unity and the apparent activation energy of creep rate was found to be about 500 kJ mol^{-1}. It means the creep deformation is due to diffusion controlled solution/precipitation. Creep rate of specimen with creep loading direction in parallel to the hot-pressing axis was determined to be higher than that in perpendicular to the hot-pressing axis. In addition, microstructural observation revealed that no cavity appeared and grain boundary glass was recrystallized during creep. X-ray diffraction (XRD) analysis confirms that needle-like Si_3N_4 grains were reoriented during creep test. These results indicate that the anisotropy of creep rate results from the disparity in the rate of solution–reprecipitation of grains rather than that in diffusion through the grain boundary, which is dependent on the preferred orientation of the needle-like grains.

1. Introduction

It is well known that α-Si_3N_4 dissolves and reprecipitates in the presence of a liquid phase as elongated needle-like grains due to the preferred grain growth along the c-axis of β-Si_3N_4 [1]. Thus, the hot pressing of silicon nitride introduces a preferred orientation such that the basal poles of β-Si_3N_4 grains lie perpendicular to the pressing direction. Also it produces the anisotropy of orientation-dependent mechanical property as reported in earlier studies [2–6].

The grain rotation and preferred nucleation or grain growth contribute to the texture development in hot-pressed β-Si_3N_4. Thus, the preferred orientation of the elongated grains result in a concurrent anisotropy in high-temperature creep resistance. However, the anisotropy of creep properties [7] has not been studied, since it is difficult to prepare the long specimen parallel to the hot-pressing axis. In this work, the influence of preferred orientation of needle-like grains on the creep rate was investigated with hot-pressed Si_3N_4 in compression. In addition, the creep mechanism will be discussed in relation with a grain growth to the creep loading direction during creep.

2. Experimental procedure

2.1. Sample preparation

α-Si_3N_4 powder was used to prepare the specimen. In order to obtain the grains with high aspect ratios, the sintering aids were selected as yttria excess, of which composition was 10.3 wt % Y_2O_3 and 2.3 wt % Al_2O_3. The powders were mixed in ethanol and ballmilled for 24 h. After the slurry was dried, the powder mixture was hot pressed in flowing N_2 at 1780 °C for 1.5 h under 33 MPa in a BN-coated graphite die. The sintered body was prepared as a size of $40 \times 50 \times 10$ mm plate. Two kinds of specimens for creep testing were cut in parallel and in perpendicular to the hot-pressing direction and ground into $3 \times 3 \times 8$ mm bars. These specimens had a different grain orientation, as illustrated in Fig. 1. In the present study, the parallel and perpendicular tests stand for creep tests in which specimens were creeploaded parallel and perpendicular to the hot-pressing axis, respectively.

2.2. Creep measurement

Tests were conducted under a compressive stress of 30–100 MPa at temperatures ranging from 1300 to 1400 °C for 100 h in ambient air. A true steady state was not attained in the creep test; then we took the average strain rates at 80 ~ 100 h of creep duration, since the linearity of the strain–time creep curve is satisfactory in the error range. We regarded it as an apparent steady-state creep rate. The stress exponent of creep rate, n was obtained from isothermal creep experiments at different load levels applying the following equation [8]

$$\dot{\varepsilon} = A\sigma^n \exp(-Q/RT) \quad (1)$$

where $\dot{\varepsilon}$ is a steady state creep rate, A is a constant, σ is the applied stress, R is the gas constant and T is the temperature. The activation energy for creep process,

0022–2461

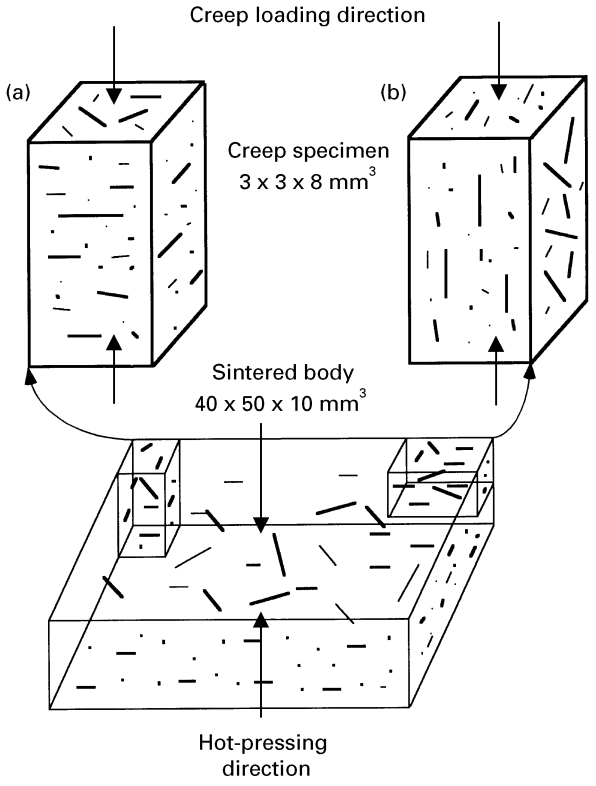

Figure 1 Schematic illustration for Si_3N_4 grain orientation and creep specimen (a) parallel and (b) perpendicular to the hot-pressing direction.

Q, was obtained from constant stress experiments using an Arrhenius plot of Equation 1.

2.3. Microstructural observation

Microstructure was examined in a scanning electron microscope (SEM) and a transmission electron microscope (TEM, H-9000, 300 kV, Hitachi). Specimens for SEM examination were prepared by electron cyclotron resonance (ECR) plasma [9] etching on planes parallel and perpendicular to the hot-pressing direction. Thin foils for TEM observation were prepared by grinding and ion milling. Textural examinations were also conducted in both the longitudinal and the transverse direction for the creep specimens. In addition, the phase analysis was performed on the grain boundary glassy phase by TEM.

2.4. X-ray diffraction (XRD) analysis

Phase analysis was carried out using XRD in both crushed specimens before and after creep test. In addition, XRD was also conducted on a plane parallel and perpendicular to the hot-pressing direction in a bulk specimen. In the XRD, the ratio of β-phase (1 0 1)/(2 1 0) peak area was used as an indication of the preferred orientation degree of elongated grains. The ratio of peak area was also estimated on the central plane perpendicular to creep-loading direction for several creep samples. The change in orientation of Si_3N_4 grains during creep was also investigated at several creep strains by comparing the ratio of (1 0 1)/(2 1 0) peak area.

3. Results and discussion

3.1. Microstructure

Fig. 2 shows the microstructures of Si_3N_4 observed from the surfaces parallel and perpendicular to the hot-pressing direction. The fully dense and fine-grained sintered body was obtained, of which grains were oriented differently to the hot-pressing direction. As shown in Fig. 2a, some grains on a surface parallel to the hot-pressing direction are seen on the hexagonal end. On the other hand, on a surface perpendicular to the hot-pressing direction, as shown in Fig. 2b, elongated grains are oriented with *c*-axis parallel to this micrograph. This result shows that needle-like β-Si_3N_4 grains are limited to growing with the preferred orientation during hot pressing.

The preferred orientations are illustrated clearly by X-ray diffraction. Both of those patterns obtained on the surfaces parallel and perpendicular to the hot-pressing direction are shown in Fig. 3. Fig. 3 reveals that β-Si_3N_4 was the only crystallographic phase and was oriented to the hot-pressing direction. To determine the degree of elongated grains' alignment, the ratio of β-phase (1 0 1)/(2 1 0) peak area was used as a parameter of grain orientation, as reported by Lee and Bowman [6]. The ratio of (1 0 1)/(2 1 0) peak area in a completely random orientation should be 1.06, according to the data of Joint Committee on Powder

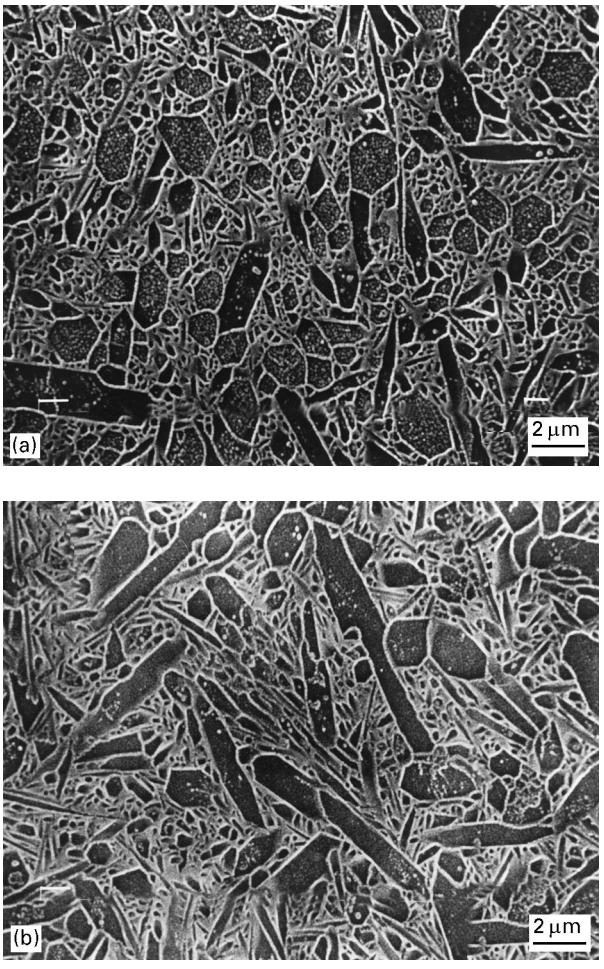

Figure 2 SEM micrographs of hot-pressed Si_3N_4 observed from surfaces (a) parallel and (b) perpendicular to the hot-pressing direction. The hot-pressing direction is horizontal in (a) and is vertical to the page in (b), respectively.

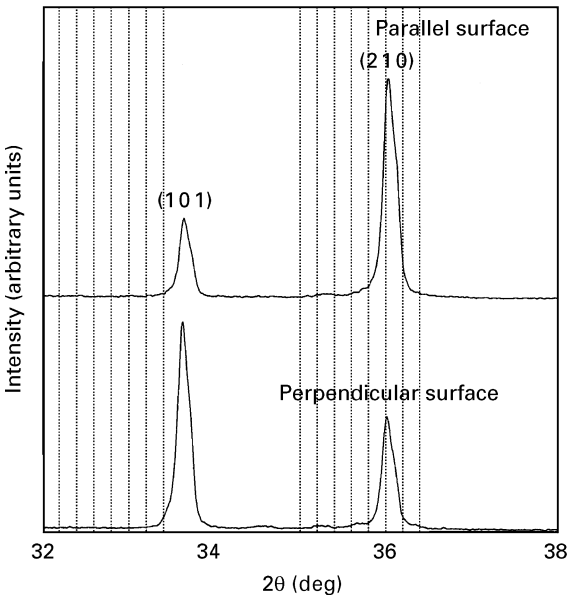

Figure 3 X-ray diffraction patterns taken on the surfaces parallel and perpendicular to the hot-pressing direction for sintered Si_3N_4.

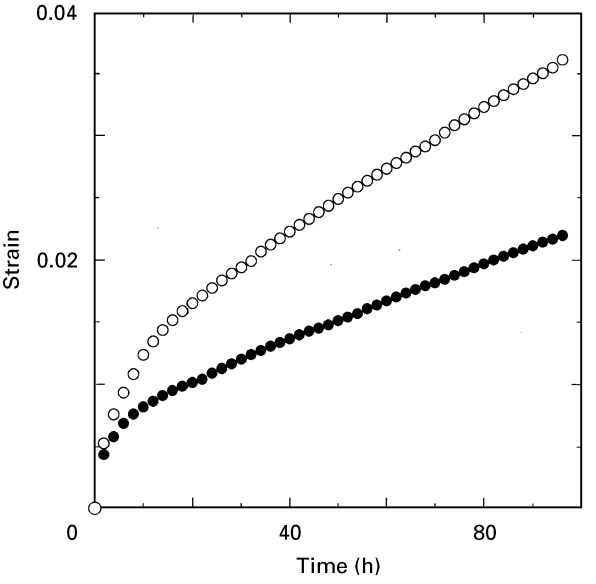

Figure 4 Creep curves of hot-pressed Si_3N_4 at 1400 °C under 75 MPa. (○) Parallel test; (●) perpendicular test.

Diffraction Standards (JCPDS) file [10]. As a result, they are 1.71 and 0.30 on the surfaces parallel and perpendicular to the hot-pressing direction, respectively. It indicates that rod-like grains develop depending on the hot-pressing direction.

3.2. Creep mechanism

Fig. 4 shows creep curves obtained at 1400 °C under 100 MPa in air. These creep curves exhibit transient creep and apparent steady-state creep after about 50 h. Total strain in the parallel test exceeds that in the perpendicular test, even though the composition and the amount of grain boundary glassy phase are almost the same. Hence, this different creep behaviour should be considered to be induced by the needle-like grain orientation in each specimen (see Section 3.4).

The dependency of applied stress on the apparent steady-state creep rate is summarized in Fig. 5. The value of the stress exponent, n is determined to be about unity in both specimens under stresses ranging from 30 to 100 MPa at 1350 °C. The microstructural observation reveals that no cavity exists in the grain boundary glassy phase. This indicates that the creep deformation is not due to cavitation but due to a diffusion-controlled mechanism.

Fig. 6. shows the dependency of temperature on the apparent steady-state creep rate determined at temperatures ranging from 1300 °C to 1400 °C under 75 MPa. The apparent activation energy for creep rate under 75 MPa is found to be about 500 kJ mol^{-1} in both parallel and perpendicular samples. This value corresponds to that for the diffusion of nitrogen ions through grain boundary glassy phase, reported by Todd *et al.* [11]. This represents the fact that the creep deformation is mainly controlled by the diffusion of nitrogen ions through the grain boundary glassy phase. Thus, the creep deformation in this study is a diffusion-controlled solution/precipitation mechanism.

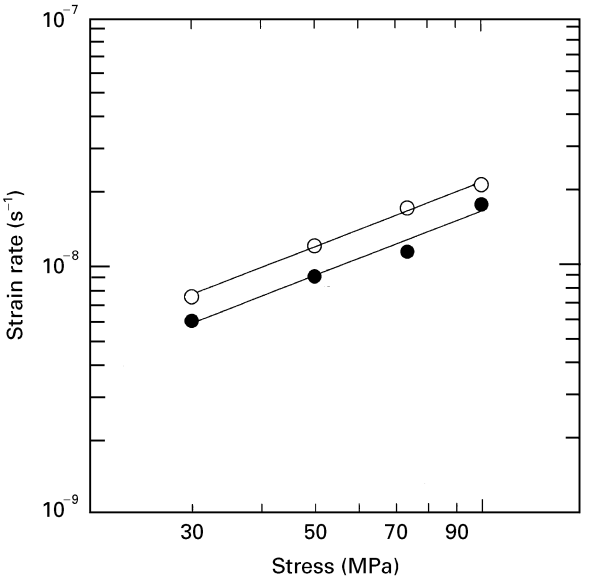

Figure 5 Stress dependencies of creep rate for Si_3N_4 parallel (○, $n = 0.86$) and perpendicular (●, $n = 0.85$) to the hot-pressing direction at 1350 °C.

3.3. Role of grain orientation in the transient creep regime

The texture development with grain orientation has been reported in previous studies [12, 13], which contain two mechanisms for preferred grain orientation, including physical grain rotation and preferential grain growth due to the stress gradient. The physical grain rotation is explained by experiments such as axisymmetric forging and plain strain compression under conditions where material has no residual α-Si_3N_4 and little grain growth occurs during the hot working [12]. It is shown that the grain rotation is a probable mechanism of texture development, considering the microstructural evidence. It is also denoted that grain reorientations in a viscous liquid can not be impeded in the tensile experiment [13]. On the

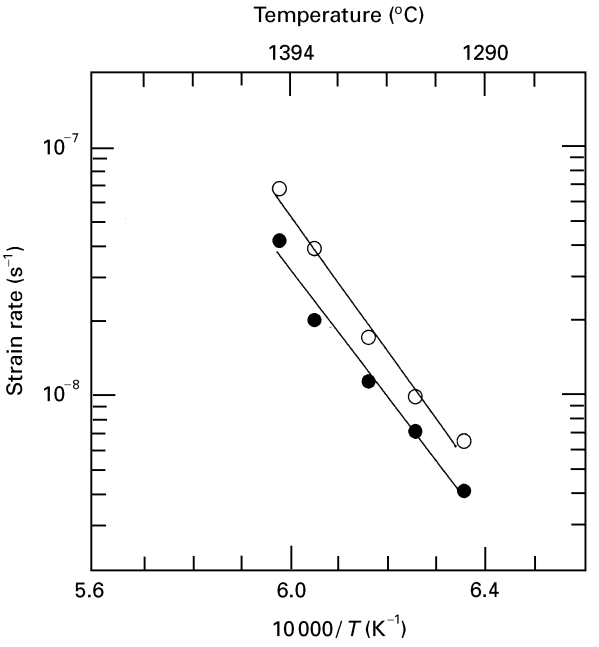

Figure 6 Temperature dependencies of creep rate for Si_3N_4 parallel (○, 520 kJ mol^{-1}) and perpendicular (●, 485 kJ mol^{-1}) to the hot-pressing direction under 75 MPa.

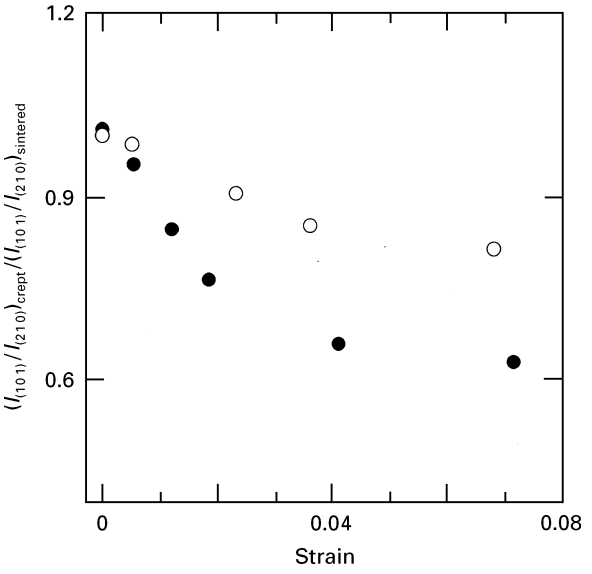

Figure 7 Change in XRD peak area ratio between (1 0 $\bar{1}$) and (2 1 0) planes for Si_3N_4 based on the values of sintered specimen as a function of creep strain. The XRD was carried out for the specimens crept at 1400 °C under 75 MPa in parallel (○) and perpendicular (●) tests.

other hand, the preferential grain growth is considered to have originated from the stress gradient for strain-induced growth onto the unconstrained grain. It is shown that the texture development due to strain-induced grain growth does not depend on the strain rate but on the total strain [13].

Fig. 7 shows the change in the ratio of β-Si_3N_4 (1 0 $\bar{1}$)/(2 1 0) peak area on a bulk specimen after creep, compared to that of a sintered specimen. It is denoted in both the materials that grains were reoriented during creep. In the perpendicular test, the ratio of (1 0 $\bar{1}$)/(2 1 0) peak area rapidly decreases in the transient creep regime and gradually decreases in the steady-state creep regime with an increase in the strain. This indicates that the physical grain rotation for texture development is a preferential mechanism to the grain growth by solution/precipitation in the transient creep regime. On the other hand, the grain growth through solution/precipitation contributes to the texture development much more than the physical grain orientation in the steady-state creep regime. It is certain that the grain rotation is due to the viscous flow, but the grain growth is mainly due to the solution/precipitation (strain-induced grain growth). However, viscous flow can redistribute the grain boundary glassy phase and thus then enables the adjacent grains Si_3N_4 to be rearranged. It suggests that the viscous flow allows the production of a physical grain rotation in the transient creep regime in the perpendicular specimen. It is because the needle-like grains are randomly distributed in two-dimensions to the creep loading direction.

On the contrary, the ratio of (1 0 $\bar{1}$)/(2 1 0) peak area in the transient creep regime is decreased more gradually in the parallel test than in the perpendicular test. It means that the physical grain rotation was prevented by the interlocking of needle-like grains in the parallel test. This result is considered to be because the creep loading was performed in the same direction to the hot-pressing axis. This is supported by the fact that the relative displacement of adjacent grains was physically limited already by grain-to-grain contact during the hot pressing. Then, it is difficult for grain rotation in the parallel test to occur. Thus, the change in the peak area ratio can occur by the preferred grain growth through the solution/precipitation of β-Si_3N_4, in which Si_3N_4 grains grow vertically to the creep loading.

The transient creep is attributed to the viscous flow from high to low local pressure on the grain boundary glassy phase [14]. The small limiting strain in compression occurs when all the intergranular phase has been squeezed out from the grain boundary under compression. A steady-state creep mechanism such as solution/precipitation may occur after the grains have started to lock each other [15, 16]. One would then expect the strain rate to decrease as the grain rotation is restricted by the interlocking of needle-like grains, and then become constant as a slower steady-state creep mechanism is dominant. The strain rate–strain relationship is shown in Fig. 8. Strain rate in the perpendicular test decreases steeply compared to that in the parallel test. The different behaviour of strain rates reflects the fact whether a large scale of physical grain rotation occurs or not. In the perpendicular test, the large scale grain rotation brings upon a steep decrease of strain rate. On the contrary, it is hard for large-scale grain orientation in the parallel test to happen. Thus, Si_3N_4 grains anisotropically grow by solution/precipitation even in the transient regime with small-scale viscous flow in the parallel test.

3.4. Differences in the steady-state creep rate

Anisotropic grain growth of β-Si_3N_4 is reported by the earlier sintering studies [6, 17]. It is explained by

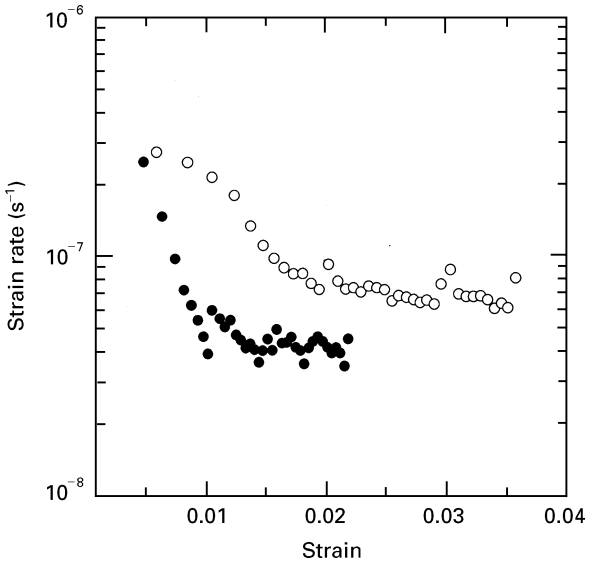

Figure 8 Strain rate of the specimens crept at 1400 °C under 75 MPa in parallel (○) and perpendicular (●) tests replotted against the strain shown in Fig. 3.

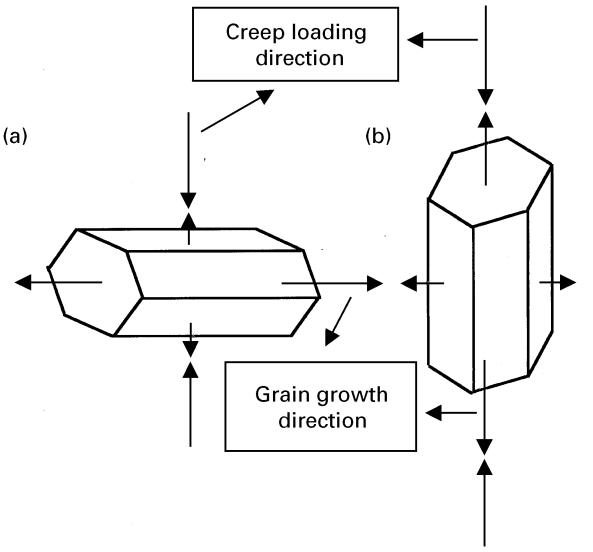

Figure 9 Schematic simplified illustration for grain orientation and anisotropic grain growth during creep process in the direction parallel (a) and perpendicular (b) to the hot-pressing axis.

understanding the growth kinetics in the ⟨0 0 1⟩ c-axis direction, which has a rounded grain surface induced by the diffusional growth without interface barrier [16]. The growth in the transverse ⟨2 1 0⟩ direction is more sluggish because of lack of growth sites. Wu *et al.* [13] reported that the significantly enhanced grain growth can occur at a much lower temperature (1550 °C) due to the assistance of a tensile plastic strain. They suggested that this enhanced growth was due to the grain coalescence and unimpingement. This mechanism is important in a highly oriented microstructure for tensile creep test. However, the microstructure of hot-pressed silicon nitride shows grain impingement to the pressing direction. In addition, the creep deformation is governed by the stress-enhanced dissolution of the contacted sites, since creep testing was conducted in compression. In this case, the grain boundary glassy phase acts as a medium through which material is transported from high stress contact sites to low stress surfaces where reprecipitation occurs.

Fig. 9 shows a schematic simplified illustration for the relationship between preferred grain orientation and creep loading direction. The creep deformation through the solution/reprecipitation can be treated in the same way as the above-mentioned sintering mechanism in the steady-state creep regime. In the parallel test, Si_3N_4 grains have already orientated in perpendicular direction to the hot-pressing axis. Thus, the solution–reprecipitation of grains to the low stress ⟨0 0 1⟩ direction occurs easily in the parallel test, since the creep stress is applied on the c-axis (2 1 0) plane, which has a deficient precipitation site; then the growth on the unconstrained (0 0 1) plane proceeds because of its sufficient precipitation site, as shown in Fig. 9a. On the other hand, the elongated Si_3N_4 grains do not sufficiently orient vertically to creep loading in the perpendicular test, in spite of the large scale grain orientation in transient creep regime. Then, it is difficult for solution–reprecipitation to occur in the unconstrained ⟨2 1 0⟩ direction in the perpendicular test, since the creep stress is loaded on the (0 0 1) plane which becomes the nucleation site in the reprecipitation of β-Si_3N_4; then the growth on the unconstrained (2 1 0) plane is prevented because of its deficient precipitation site, as shown in Fig. 9b. Thus, the solution rate of grains is lower in the perpendicular test than in the parallel test. Therefore, the creep rate in the parallel test exceeds that of the perpendicular test in the steady-state creep regime.

Considering the parallel process of solution/precipitation creep, the slower rate of either the solution–reprecipitation or the diffusion through the grain boundary will appear as a net creep rate [15, 16]. In this study, the rate-limiting step was determined to be the diffusion through the grain boundary for both (parallel and perpendicular) specimens (discussed in Section 3.2). It is reasonable that the rate of diffusion step is almost the same in both of specimens, since the composition and the amount of grain boundary glassy phase are almost the same. However, the net creep rate can be increased with an increase in the rate of the solution–reprecipitation step even in the parallel creep process. As above mentioned, the rate of the solution–reprecipitation step is determined to be lower in the perpendicular test than that in the parallel test. Thus, the creep rate in the perpendicular test exhibits a lower value than that in the parallel test, even though the rate-controlling step is diffusion through the grain boundary. Although the effect of preferred orientation on the creep resistance in tensile has not been investigated, the effect of grain orientation in the range of the solution/pecipitation creep should produce the opposite result to that of compression test.

The creep deformation due to solution/precipitation will enable the shape of Si_3N_4 grains to change and small grains to grow through the stress gradient. Fig. 10 shows the microstructural change in the

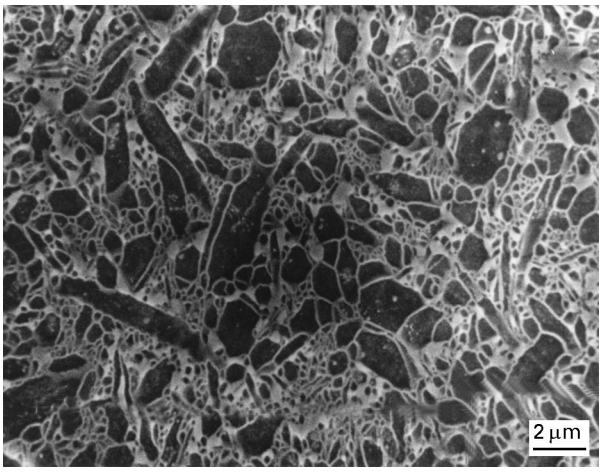

Figure 10 SEM micrograph of cross-sectional plane perpendicular to the creep loading direction from Si_3N_4 perpendicular to the hot pressing direction crept at 1400 °C under 75 MPa.

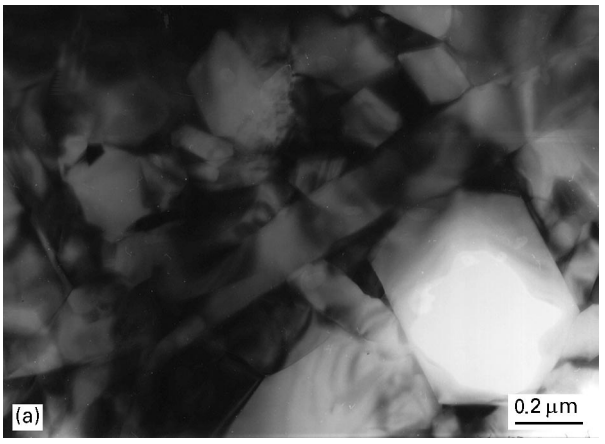

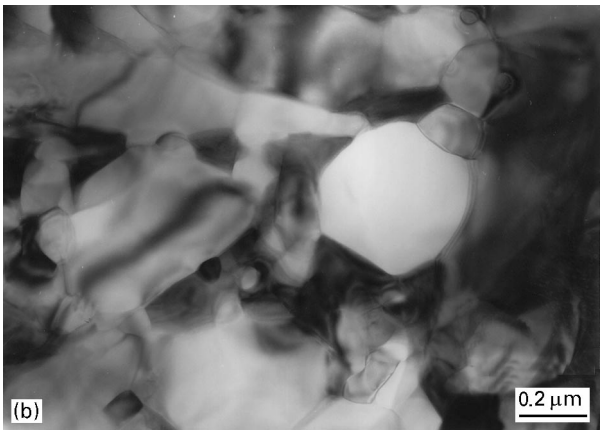

Figure 11 TEM micrographs of Si_3N_4 perpendicular to the hot-pressing direction (a) sintered and (b) cross-sectional plane perpendicular to the creep loading direction crept at 1400 °C under 75 MPa.

perpendicular test after creep. It is certain that grain boundary glass is squeezed out at two grain junctions and coalesces at the triple junction of small grains because of the viscous flow in the transient creep regime. It is, however, difficult to recognize the grain growth and shape change in specimens before and after creep, since the conditions for creep experiments are chosen such that little grain growth of the Si_3N_4 materials is observed at temperatures lower than 1400 °C; then the maximum strain of the creep deformation is still smaller than 0.06. However, it is clear that the number of small grains is decreased in the creep specimen compared to that in the sintered specimen (see Fig. 2a). This shows that the grain growth occurs by the solution/precipitation creep.

The shape change in the faceted grains is demonstrated clearly by TEM micrograph of cross-sectional plane perpendicular to the creep loading direction, as shown in Fig. 11. It is shown that faceted Si_3N_4 grains were grown rounded in the creep specimen. The shape change in elongated grains along the unconstrained direction is evident and substantiates the results given by the small change in the ratio of (1 0 1)/(2 1 0) peak area at steady-state creep regime. It suggests that grains grow and deform along the transverse direction through the stress gradient to the compression, and the creep deformation is due to the solution/precipitation. In addition, this is evidence that the creep rate in the material with anisotropically-grown grains containing glassy phase can be determined by the rate of the solution–reprecipitation step to the unconstrained direction, as illustrated in Fig. 9.

4. Conclusions

1. The stress exponent of creep rate was determined to be nearly unity, and apparent activation energy in both parallel and perpendicular tests was found to be about 500 kJ mol^{-1}, which suggests that creep deformation is mainly controlled by diffusion through the grain boundary glassy phase.
2. The creep deformation rate of specimen loading in the direction parallel to the hot pressing, was determined to be higher than that perpendicular to the hot pressing.
3. The anisotropy of creep rate to the creep loading direction in specimens which have the preferred orientation of elongated grains results from the disparity in the rate of the solution–reprecipitation step.

Acknowledgements

The authors are grateful to Professor F. F. Lange of the University of California at Santa Barbara for helpful discussion. Thanks also to Dr N. Kamiya of Toyota Central R&D Labs. Inc. for plasma etching of SEM specimen, and Professor T. Yano of Tokyo Institute of Technology for using TEM.

References

1. D.-D. LEE, S.-J. L. KANG and D.-Y. YOON, *J. Amer. Ceram. Soc.* **71** (1988) 805.
2. R. KOSSOWSKY, *J. Mater. Sci. Lett.* **8** (1973) 1603.
3. K. NUTTAL and D. P. THOMPON, *ibid.* **9** (1974) 850.
4. F. F. LANGE, *J. Amer. Ceram. Soc.* **56** (1973) 518.
5. J. E. WESTON, *J. Mater. Sci.* **15** (1980) 1568.
6. F. LEE and K. BOWMAN, *J. Amer. Ceram. Soc.* **75** (1992) 1748.
7. X. WU and I-W. CHEN, Unpublished results, presented at the 93rd Annual Meeting of the American Ceramic Society, Cincinnati, Oh; Apr. 30–May 4 (1995).

8. M. K. FERBER and M. G. JENKINS, *J. Amer. Ceram. Soc.* **75** (1992) 2453.
9. A. SUDA, I. TAJIMA, M. ISHII, M. TADA, Y. UKYO and S. WADA, *J. Ceram. Soc. Jpn.* **101** (1993) 217.
10. JCPDS file set 33–1160.
11. J. A. TODD and Z.-Y. XU, *J. Mater. Sci.* **24** (1989) 4443.
12. F. LEE and K. BOWMAN, *J. Amer. Ceram. Soc.* **77** (1994) 947.
13. X. WU and I-W. CHEN, *ibid.* **75** (1992) 2733.
14. J. R. DRYDEN, D. KUCEROVSHY, D. S. WILKINSON and D. F. WATT, *Acta Metall.* **37** (1989) 2007.
15. R. RAJ and C. K. CHUNG, *ibid.* **29** (1981) 159.
16. F. WAKAI, *ibid.* **42** (1994) 1163.
17 M. HWANG, T. Y. TIEN and I-W. CHEN, in "Sinterng 87" Vol. 2, edited by S. Somiya, M. Shimada, M. Yoshimura and R. Watanabe, Tokyo, Japan, November, 1987 (Elsevier Applied Science, London, 1988) p. 1034.

Received 18 October 1995
and accepted 20 January 1997